Twisted optical molasses for all-optical atomic cooling and trapping

A. R. Carter[1,2] and M. Babiker[2]
[1]*Department of Physics, University of Sheffield, Sheffield S3 7RH, United Kingdom*
[2]*Department of Physics, University of York, Heslington, York YO10 5DD, United Kingdom*
(Received 25 October 2007; published 1 April 2008)

We explain how a proper specification of the spatial field distribution and angular momentum content of a twisted light beam propagating in an arbitrary direction can be made using appropriate transformations. Such transformations are needed whenever a light beam is to be combined with other similar beams propagating in specified directions. The transformation procedure greatly facilitates the evaluations of the radiation forces acting on atoms subject to an arbitrary set of twisted light beams. It allows atomic trajectories in one-, two-, and three-dimensional optical molasses configurations to be correctly evaluated. We find that multiple twisted beams offer a flexible means of controlling the motion of atoms, but there are notable features attributable only to the orbital optical angular momentum property of the twisted light. Under suitable conditions, atoms can be decelerated and ultimately made to congregate in specific regions of space. The implications of this for all-optical atomic cooling and trapping using twisted light are pointed out and discussed.

DOI: 10.1103/PhysRevA.77.043401 PACS number(s): 37.10.De, 37.10.Vz, 32.80.Wr

I. INTRODUCTION

Experimental investigations on the mechanical action of laser light on matter, especially the acceleration and the trapping of micron-sized particles in optical potential wells, were carried out by Ashkin [1]. Since then much theoretical and experimental work has studied radiation forces and, in particular, the near-resonant interaction of laser light with atoms and ions [2–4].

The simplest features can be understood by considering a two-level system, representing an atom in an electromagnetic field. If the field is tuned such that it is at or near resonance with the atom, the radiation force can be considered as the sum of two distinct contributions: the dipole force associated with the nonconformity of the field distribution and the dissipative force arising from the absorption and reemission of photons by the atom. The dipole force can be used to trap atoms [5] and the dissipative force to cool or heat the atomic motion [6].

Much of the theoretical work on laser cooling and trapping has assumed light modes with plane-wave fronts. In the early 1990s, Allen *et al.* mathematically demonstrated that Laguerre-Gaussian (LG) light possesses a well-defined quantized orbital angular momentum $l\hbar$ [7] with l an integer. The orbital angular momentum is a previously overlooked property of light. It arises from the azimuthal phase dependence of the field distribution and is distinct from spin angular momentum. Circularly polarized LG light possesses a nonzero spin as well as orbital angular momenta. Linearly polarized LG modes maintain the property of orbital angular momentum.

It has been shown that light endowed with orbital angular momentum, known as twisted light, induces a torque on particles as a result of the transfer of the orbital angular momentum to the particle [8,9]. It has also been established that for electric dipole-allowed processes a transfer of orbital angular momentum occurs only between the light and the center-of-mass motion. Consideration of a two-level atom in the field of a twisted beam in the saturation limit results in a torque of $l\hbar\Gamma$ being exerted on the atom, where Γ is the width of the upper state [8]. LG beams also produce rotational motion on matter in the bulk and this has led to the application of twisted beams in optical spanners [10], which are essentially the rotational forms of optical tweezers [11], and more recently pattern formation in optically trapped nanoparticles [12–14].

In the mid 1990s Allen *et al.* considered atom dynamics in multiple Laguerre-Gaussian beams [15]. This theoretical treatment of the influence of multiple beams on atomic motion dealt with counterpropagating beams in which one of the pair was constructed by switching the sign of the axial wave vector $\mathbf{k}$. As pointed out in Ref. [16], the resulting forces are thus due to the combination of a beam and its retroreflection. There is need, however, to consider the general case in which independent beams can be traveling in any desired direction and so be able to determine the net forces due to any set of multiple beams which influence atomic motion.

We determine the field distributions of each independent beam by transforming the original beam using rigid body transformations. In order to discuss optical molasses in one, two, and three dimensions we apply coordinate transformations on the standard form of a twisted beam propagating in the z direction. The total force on an atom due to a given set of beams can therefore be determined with reference to the beam specified in the original Cartesian axes.

The rest of this paper is structured as follows. In Sec. II we introduce the steady state forces due to a twisted beam and consider the dipole potential due to a single beam. We then set up a set of coordinate transformations from which a beam propagating in an arbitrary direction can be considered in terms of the original Cartesian axes. In Sec. III we describe the motion of a Mg^+ ion subject to the combined effects of the forces due to all the counterpropagating beams. This requires the numerical solutions of the classical equations of motion, subject to initial conditions. Our main conclusions are outlined in Sec. IV.

II. FORMALISM

The essential features of a twisted beam, at a general position $\mathbf{R}=(r,\phi,z)$ in cylindrical polar coordinates, are the phase $\Theta_{klp}(\mathbf{R})$ and the Rabi frequency $\Omega_{klp}(\mathbf{R})$. Ignoring beam curvature, these are written as

$$\Theta_{klp}(\mathbf{R}) = l\phi + kz, \tag{1}$$

$$\Omega_{klp}(\mathbf{R}) \approx \Omega_0\left(\frac{r\sqrt{2}}{w_0}\right)\exp(-r^2/w_0^2)L_p^{|l|}\left(\frac{2r^2}{w_0^2}\right), \tag{2}$$

where the beam has a frequency ω, axial wave vector $\mathbf{k}$, and quantum numbers l and p. These forms are obtainable from the corresponding standard expressions for the Laguerre-Gaussian beam in the limit $z \ll z_R$ where z_R is the Rayleigh range [15], and setting $w(z)=w_0$.

Using density matrix techniques, the steady state forces on an atom of velocity $\mathbf{V}=\dot{\mathbf{R}}$ are in general found to be

$$\langle \mathbf{F}_{\text{diss}}\rangle_{klp} = 2\hbar\Gamma\Omega_{klp}^2(\mathbf{R})\left(\frac{\nabla\Theta_{klp}(\mathbf{R})}{\Delta_{klp}^2(\mathbf{R},\mathbf{V})+\Gamma^2+2\Omega_{klp}^2(\mathbf{R})}\right), \tag{3}$$

$$\langle \mathbf{F}_{\text{dipole}}\rangle_{klp} = -2\hbar\Gamma\Omega_{klp}(\mathbf{R})\,\nabla\,\Omega_{klp}(\mathbf{R}) \times\left(\frac{\Delta_{klp}(\mathbf{R},\mathbf{V})}{\Delta_{klp}^2(\mathbf{R},\mathbf{V})+\Gamma^2+2\Omega_{klp}^2(\mathbf{R})}\right). \tag{4}$$

The dissipative force $\langle \mathbf{F}_{\text{diss}}\rangle$ represents the force due to the absorption and reemission of the light by the atom; and the dipole force $\langle \mathbf{F}_{\text{dipole}}\rangle$ arises from the nonconformity of the field distribution. The dynamic detuning is defined as

$$\Delta_{klp}(\mathbf{R},\mathbf{V}) = \Delta_0 - \mathbf{V}\cdot\nabla\Theta_{klp}(\mathbf{R}), \tag{5}$$

where $\Delta_0=\omega-\omega_0$ is the static detuning, with $\hbar\omega_0$ the level energy separation of the two-level atom and ω the frequency of the light. Γ is the half-width of the upper quantum atomic state.

The static component of the dipole force can be derived from a potential

$$\langle U(\mathbf{R})\rangle_{klp} = \frac{\hbar\Delta_0}{2}\ln\left[1+\frac{2\Omega_{klp}^2(\mathbf{R})}{\Delta_0^2+\Gamma^2}\right] \tag{6}$$

such that $\langle F_{klp}^0\rangle=-\nabla\langle U(\mathbf{R})\rangle_{klp}$. For red detuned light $\Delta_0<0$, the potential exhibits a minimum in the high intensity region of the beam, trapping atoms in the strong field regions. For blue detuned light $\Delta_0>0$, atoms are trapped in the dark regions of the beam where the intensity is low. For the Laguerre-Gaussian mode $l=1$ and $p=0$ the potential on a stationary atom is

$$\langle U\rangle_{k10} = \frac{\hbar\Delta_0}{2}\ln\left[1+\frac{2\Omega_{k10}^2(\mathbf{R})}{\Delta_0^2+\Gamma^2}\right]. \tag{7}$$

At the beam waist $z=0$, the minimum occurs at a radial distance given by

$$r_0 = w_0/\sqrt{2}. \tag{8}$$

For a beam propagating along the z axis the locus of potential minima in the xy plane is given by a circle whose equation is

$$x^2+y^2 = r_0^2. \tag{9}$$

If we now expand the potential in powers of $(r-r_0)$ and restrict ourselves to the parabolic approximation, then the potential becomes

$$\langle U\rangle_{k10} \approx U_0 + \frac{1}{2}\Lambda_{k10}(r-r_0)^2, \tag{10}$$

where the potential depth U_0 is given by

$$U_0 = \frac{1}{2}\hbar\Delta_0\ln\left[1+\frac{2\Omega_{k10}^2(r_0)}{\Delta_0^2+\Gamma^2}\right] \tag{11}$$

and the effective elastic constant of the quasisimple harmonic motion Λ_{k10} by

$$\Lambda_{k10} = \frac{4\hbar|\Delta_0|}{\Delta_0^2+2e^{-1}\Omega_{k00}^2+\Gamma^2}\left(\frac{e^{-1}\Omega_{k00}^2}{w_0^2}\right). \tag{12}$$

If the atom's kinetic energy is less than $|U_0|$, then it is considered trapped. As the atom falls into the optical trap it will oscillate about $r=r_0$ with an angular frequency of $\sqrt{\Lambda_{k10}/M}$, where M is the mass of the atom.

In order to consider multiple beams in various configurations in space, it is expedient to express the forces in Cartesian coordinates $\mathbf{R}=(x,y,z)$. We therefore recast Eqs. (3) and (4) in Cartesian form

$$\langle \mathbf{F}_{\text{diss}}(\mathbf{R},\mathbf{V})\rangle + \langle \mathbf{F}_{\text{dipole}}(\mathbf{R},\mathbf{V})\rangle = \langle F_x\rangle\hat{\mathbf{x}} + \langle F_y\rangle\hat{\mathbf{y}} + \langle F_z\rangle\hat{\mathbf{z}}. \tag{13}$$

A twisted beam propagating in a general direction can then be constructed by considering a rotation in the xz plane about the y axis by an angle θ and then a further rotation about x by an angle ψ. This leads to the transformation matrix

$$\mathbf{T}(\theta,\psi) = \begin{bmatrix} \cos(\theta) & 0 & \sin(\theta) \\ -\sin(\theta)\sin(\psi) & \cos(\psi) & \cos(\theta)\sin(\psi) \\ -\sin(\theta)\cos(\psi) & -\sin(\psi) & \cos(\theta)\cos(\psi) \end{bmatrix}, \tag{14}$$

which is employed to transform the original coordinates into our new frame of reference.

The procedure described above can be utilized by a suitable choice of the angles θ and ψ to obtain the force distribution due to a twisted light beam propagating in any chosen direction. The obvious applications to be considered are those corresponding to the conventional geometric arrangements, specifically those involving one-dimensional (1D), two-dimensional (2D), and three-dimensional (3D) twisted beam optical molasses.

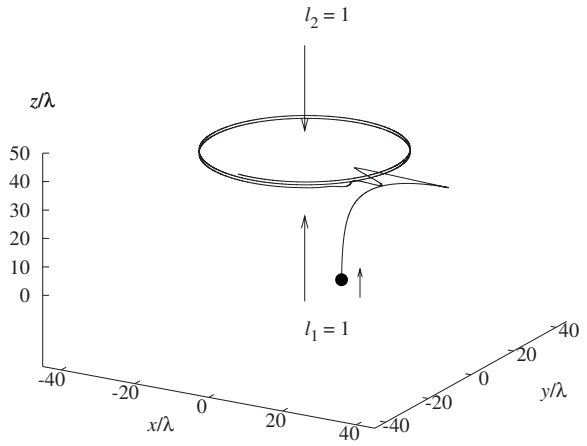

FIG. 1. The trajectory of a Mg^+ ion in 1D counterpropagating twisted beams with $l_1=l_2=1$ and $p_1=p_2=0$. The initial velocity of the atom is $v_z=5$ m s^{-1}. The initial position, as in subsequent figures, is indicated by a full circle.

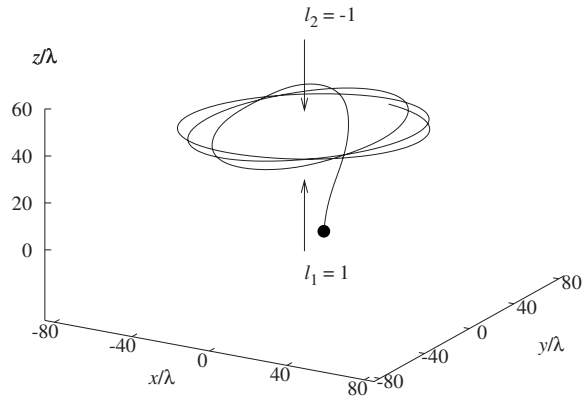

FIG. 2. As in Fig. 1 but with $l_1=-l_2=1$ and $p_1=p_2=0$.

III. ORTHOGONAL COUNTERPROPAGATING TWISTED LIGHT BEAMS

We have determined the motion of magnesium ions Mg^+ in the fields of counterpropagating twisted light beams in three configurations. Mg^+ has a suitable transition that can be closely tuned to the frequency of the light. The Mg^+ mass is $M=4.0\times10^{-26}$ kg, the transition wavelength is $\lambda=280.1$ nm, and its half-width is $\Gamma=2.7\times10^8$ s^{-1}.

We consider red detuned light to induce trapping in areas of high intensity $\Delta_0=-\Gamma$. The full dynamic detuning given in Eq. (5) is used in the model. The Laguerre-Gaussian "doughnut" mode $l=\pm1$ and $p=0$ is used throughout. The equation of motion for the Mg^+ ion is

$$M\frac{d^2}{dt^2}\mathbf{R}(t)=\sum_i\{\langle\mathbf{F}_{\text{diss}}\rangle+\langle\mathbf{F}_{\text{dipole}}\rangle\}_i, \tag{15}$$

where the summation accounts for the individual radiation force contributions from the beams present.

A. 1D twisted optical molasses

We begin by considering the simple one-dimensional (1D) configuration in which a pair of counterpropagating LG beams is set up propagating along the z axis. One of the beams is specified in the negative z direction using the transformation matrix (14) with $\theta=\pi$ and $\psi=0$. It can be checked that the resulting equations are not those due to a mirror reflection of the original beam.

Figure 1 shows the trajectory of the Mg^+ ion in the field of two counterpropagating beams, beam 1 propagating in the positive z direction and beam 2 in the negative z direction, with $l_1=l_2=1$. The Mg^+ ion is initially at the radial position $r=10\lambda$ with an initial velocity of $\mathbf{V}(0)=5$ m s^{-1} $\hat{\mathbf{z}}$. The duration of the trajectory is $5\times10^5\Gamma^{-1}$. It can be seen that the atom slows down to a halt in the z direction, corresponding to the axial cooling, while in its in-plane motion the ion is attracted toward the region of high beam intensity located at a radius $r_0=w_0/\sqrt{2}$. Initially the ion exhibits a quasiharmonic vibrational motion in its in-plane motion, which is rapidly dampened until the atom falls into the bottom of the potential well. For the two beams in this configuration the effective elastic constant is twice that of the one beam case given in Eq. (12), which implies that the vibrational frequency of the 1D configuration here is

$$\nu=\frac{1}{2\pi}\left(\frac{8\hbar|\Delta_0|e^{-1}\Omega_{k00}^2}{Mw_0^2[\Delta_0^2+2e^{-1}\Omega_{k00}^2+\Gamma^2]}\right)^{1/2}. \tag{16}$$

This yields $\nu\approx1.2\times10^4\Gamma$ using the above parameters, which is in agreement with the frequency of the oscillations deduced from the in-plane motion.

Clearly, once the Mg^+ ion is trapped axially it rotates clockwise about the common beam axis with a constant angular velocity. Therefore, there is zero net torque in this case. This can be easily understood if we consider the combined torques in the saturation limit for the two beams $|\langle\mathbf{T}\rangle|\approx l_1\hbar\Gamma-l_2\hbar\Gamma=0$. Inverting the signs of the azimuthal indices such that $l_1=l_2=-1$ causes the circular in-plane motion to be anticlockwise.

Inverting the sign of the azimuthal index of one of the beams, i.e., $l_1=-l_2=1$, results in a nonzero torque. The combined torques in the saturation limit for the two beams in this case give $|\langle\mathbf{T}\rangle|\approx l_1\hbar\Gamma-l_2\hbar\Gamma=2\hbar\Gamma$. The trajectory of the magnesium ion in this setup is shown in Fig. 2. The duration of the trajectory is $5\times10^4\Gamma^{-1}$. As before, the Mg^+ ion is trapped axially between the two beams and it rotates clockwise about the common beam axis. Once more, the atom's in-plane motion is attracted toward the region of high beam intensity. However, due to the net torque and the velocity dependence of the potential it is seen that the motion does not follow a path defined by the regions where the potential is a minimum. The long-time behavior constitutes a uniform circular motion, as can be deduced from Fig. 3, exhibiting the evolution of the velocity components. The cooling in the axial direction is evident in the rapid decrease of the axial velocity component and the uniform circular motion is evident in the near equality (after a long time has elapsed) of the two in-plane velocity components.

Where there is circular motion of the Mg^+ ion of radius r_0 this constitutes an electric current source of micron size. For orientation as to orders of magnitude, we have a current i

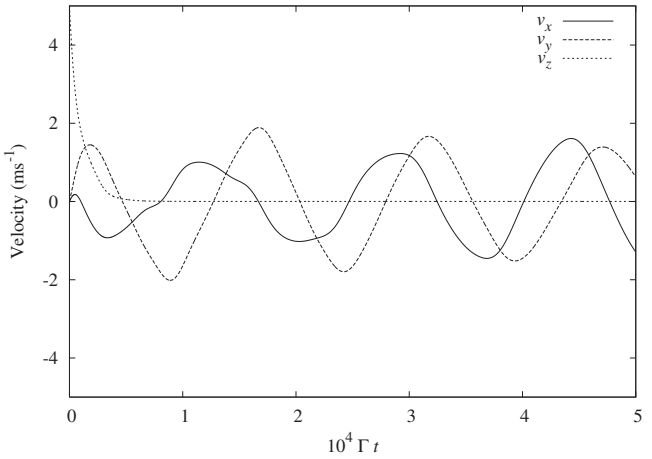

FIG. 3. The time variations of the velocity components of a Mg^+ ion in 1D counterpropagating twisted beams with $l_1=-l_2=1$ and $p_1=p_2=0$, where v_z is seen to rapidly decrease to zero, while v_x and v_y indicate a tendency toward a uniform circular motion after an initial variation.

$\approx e/\tau$, where $\tau=2\pi r_0/v_s$, with $v_s\approx 10$ m s^{-1}the long-time speed and $r_0\approx w_0=35\lambda$. A straightforward evaluation leads to a current of the order of pA if a single ion is involved and a nA for 10^3 ions and to a mA for 10^6 ions. The Mg^+ ions are assumed to be precooled with a distribution of velocities. Once the LG beams are switched on, a large fraction of the ions can be made to proceed toward the optical well which is set up by the twisted molasses beams. Once trapped they will continue to revolve in the circular orbit, as described above. There would also an associated magnetic field whose magnitude and distribution can be easily evaluated, as for the case of a standard circular current loop.

B. 2D twisted optical molasses

A two-dimensional (2D) twisted molasses configuration is now constructed by the introduction of a second pair of twisted beams perpendicular to the original pair. The pairs could have different width parameters w_0 and w_0'. In addition

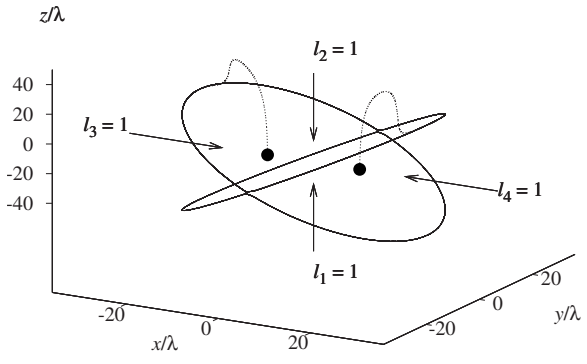

FIG. 4. The trajectories of two Mg^+ ions starting at different positions in 2D counterpropagating twisted beams where $l_i=1$ and $p_i=0$, $i=1-4$. The initial velocity of each ion is $v_z=5$ m s^{-1}. It is seen that each ion ends up motionless at points lying on the locus of lowest minima, corresponding to the two oblique orthogonal circles.

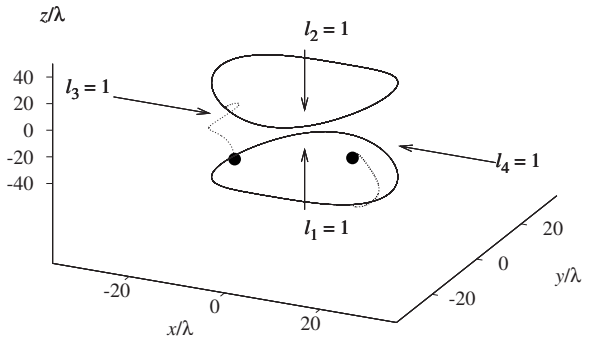

FIG. 5. As in Fig. 4 but the pair of counterpropagating beams along the x axis have $w_0'=35\lambda$ while the pair along z have $w_0'=25\lambda$. The ion ends up motionless on the locus of lowest minima, corresponding to the two loops.

to this difference, this configuration corresponds to the conventional two-dimensional molasses configuration, but here the four beams are all twisted.

For this setup the potential minima are situated along the locus of spatial points defined simultaneously by two equations $x^2+y^2=w_0^2/2$ and $y^2+z^2=w_0'^2/2$. The locus of spatial points where the dipole potential is minimum can be described by the parametric equations [18]

$$x(u)=(w_0'/\sqrt{2})\cos u,\quad y(u)=(w_0'/\sqrt{2})\sin u,$$

$$z(u)=\pm\sqrt{w_0^2/2-(w_0'/2)\sin^2 u}. \tag{17}$$

For $w_0'=w_0$ the equations describe two orthogonal oblique circles representing the intersection curves of two cylinders of radii $w_0/\sqrt{2}$. In this configuration trapping of the Mg^+ ions will occur at points lying on one of the two oblique circles as determined by the initial conditions. An ensemble of Mg^+ ions with a distribution of initial positions and velocities will populate the two circles, producing two orthogonal, essentially static Mg^+ ion loops (see Fig. 4). Associated with this system of charges would be a Coulomb field whose spatial distribution for ions uniformly distributed in the rings can be easily evaluated.

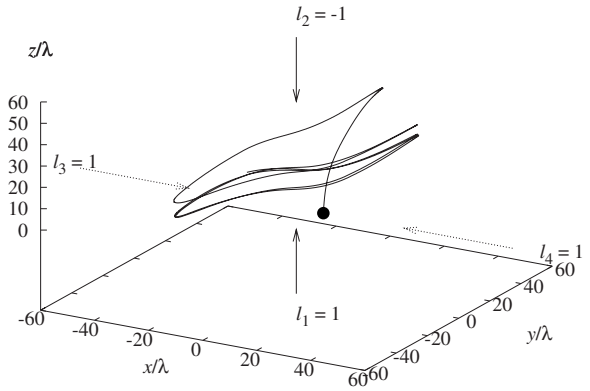

FIG. 6. Projection of the trajectory of a Mg^+ ion in the xy plane in 2D counterpropagating twisted beams with $l_1=-l_2=1$ along z (perpendicular to the page) and $l_3=l_4=1$ along x, and $p_i=0$.

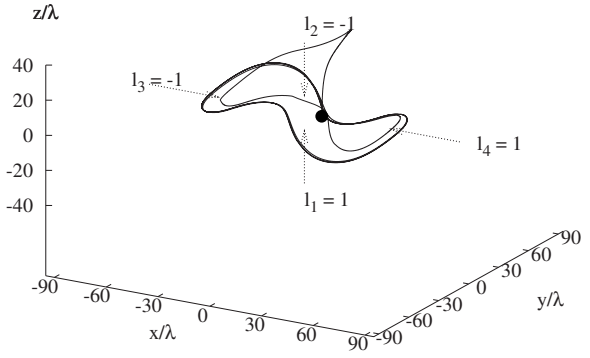

FIG. 7. The trajectory of a Mg^+ ion in 2D counterpropagating LG beams, where the arrows indicate direction of beam propagation and their respective l values; all beams have $p=0$.

For $w_0' \neq w_0$ then the locus of spatial points where the dipole potential is minimum becomes two circular loops separated from one another. Figure 5 shows the trajectory of two Mg^+ ions in a 2D configuration where $w_0=25\lambda$ and $w_0'=35\lambda$, the two loops representing the loci of potential minima. As in the case of $w_0=w_0'$, ions populate the two loops resulting in two separate Mg^+ ion loops. Changing the magnitudes of l has a similar effect to varying the value of w_0 for the pairs of beams.

We now consider the 2D case where one or both of the pairs of beams generates a torque. The simplest configuration to be considered here is the one in which the pair of beams along the z axis provide a net torque, with $l_1=-l_2=1$, and the pair along x provide zero net torque, with $l_3=l_4=1$. Figure 6 displays the trajectory of a Mg^+ ion, initially at the radial position $r=10\lambda$ and with an initial velocity $\mathbf{V}_z(0)=5$ m s^{-1}, projected on the xy plane. As in the previous cases, the ion is axially cooled along the z direction, becoming trapped in the xy plane. However, the in-plane motion is more complex than before with its trajectory tracing out a path that resembles a hysteresis figure. The ion seeks to follow a trajectory in the region of potential minima, while responding to the torque arising from the beams along the z axis which causes the ion to be displaced from the potential minimum in a sling-shot-like motion.

If both pairs of beams generate a torque, then the resulting trajectory shape resembles a hysteresis figure in a fixed inclined plane, as seen in Fig. 7. The ion is responding to the combined effects of orthogonal torques and axial cooling forces.

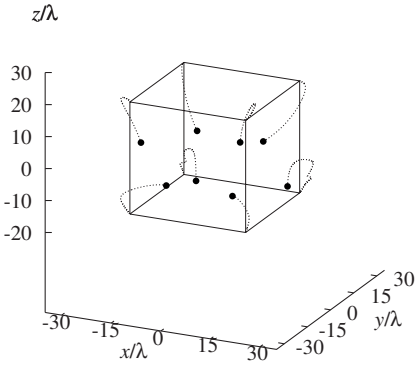

FIG. 8. The trajectories of a Mg^+ ion in 3D counterpropagating LG beams for $l_i=1$ and $p_i=0$, $i=1-8$. The initial velocity of each of the ions is $v_z=5$ m s^{-1}. It is seen that the atom ends up motionless at points lying on the corners of the cube of side w_0.

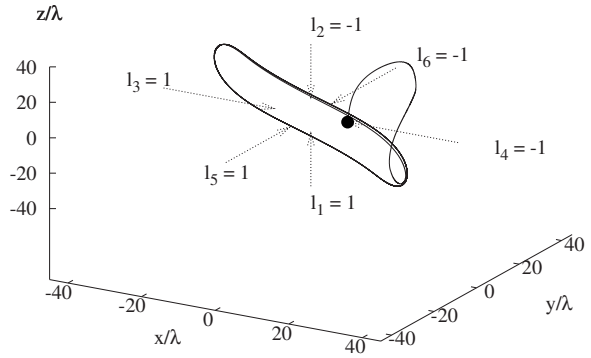

FIG. 9. The trajectory of a Mg^+ ion in 3D counterpropagating LG beams, where the arrows indicate direction of beam propagation and their respective l values; all beams have $p=0$.

C. 3D twisted optical molasses

The final case considered here is the three-dimensional (3D) configuration in which a third pair of counterpropagating beams is added to the 2D configuration, orthogonal to the plane containing the original beams. All six beams have an azimuthal index $l=1$. In this case, the deepest potential minima are located at eight discrete points defined by the coordinates: $x=\pm(w_0/2)$, $y=\pm(w_0/2)$, $z=\pm(w_0/2)$. These coincide with the eight corners of a cube of side w_0, centered at the origin of coordinates.

Figure 8 shows the trajectory of eight Mg^+ ions positioned at different initial positions, each with an initial velocity $\mathbf{V_z}(0)=1$ m s^{-1}, in the 3D case. Each ion is seen to end up at one of the eight discrete points where the dipole potential is minimum, where it remains essentially motionless. There is no net torque on this system.

As in the cases of 1D and 2D configurations we have found that when each counterpropagating pair in the 3D configuration provides a nonzero torque resulting in a nonzero net torque on the system the atom is trapped within a loop in which it moves. This can be seen in Fig. 9 where each pair consists of a $l=1$ beam and a $l=-1$ beam. As in the 2D case the ion seeks to follow a trajectory in the region of potential minima, while responding to the torque arising from the pairs of counterpropagating beams along each axis, which causes the ion to be perturbed from the potential minimum in a sling-shot-like motion.

IV. CONCLUSIONS

Ordinarily, optical molasses cannot be used as an atom trap. If we consider a one-dimensional configuration of two coaxial plane waves propagating in opposite directions to one another, then it is not possible to trap an atom in all directions between the two beams. If the atom is displaced from the center there is no restoring radial force to keep the atom trapped.

For optical molasses using twisted beams such as Laguerre-Gaussian light it is possible to completely trap atoms. Unlike Gaussian beams, Laguerre-Gaussian light has a radial force which can be employed to keep an atom trapped within the field of the beams.

We have shown that using twisted beams it is possible, in principle, to trap atoms in well defined regions of space. Using various configurations we have shown that by all-optical means it is possible to create nanoscale atomic and ionic rings that may either be static or in motion. These rings will produce highly localized electric and magnetic fields. The positioning and scale of the rings can be controlled by varying the parameters l and w_0 of the beams.

Using a 3D configuration we have shown that it is possible to trap atoms in eight discrete points that form the eight corners of a cube whose dimensions represent the width of the beams in the configuration. We suggest that by using a suitable repetition of the twisted molasses arrangement a larger lattice could be constructed. This lattice could then be usefully exploited in the study of coupled Bose-Einstein condensates and in quantum information processing. A system of cold atoms entering the twisted optical molasses region would automatically become trapped in the eight corners of the cube, as shown in Fig. 8. Evaporative cooling techniques can then be followed to produce the BECs [17]. Progressively stronger coupling between trapped BECs is achievable by a reduction in the value of w_0. The twisted beam environment offers flexibility in that one can choose at will various parameters, for example, controlling the distances between the trapping sites, while the depth of the confining potential is controlled by the light intensity and the detuning. There are also possibilities, as in plane wave optical lattices, for trapping a single atom at each site, in which case the arrangement could be used for quantum information processing [19]. The procedure for quantum protocols would be the same as that for conventional ion traps where quantum information processes have been studied in some depth [20]. The main advantage here is that the trapping as well as processing would be all optical.

ACKNOWLEDGMENTS

This work was supported by the U.K. Engineering and Physical Sciences Research Council (EPSRC) Grant No. GR/R15269/01. The authors are grateful to the EPSRC for this grant.

[1] A. Ashkin, Phys. Rev. Lett. **24**, 156 (1970).
[2] V. S. Letokhov and V. G. Minogin, *Laser Light Pressure on Atoms* (Gordon and Breach, New York, 1987).
[3] A. P. Kazantsev, G. I. Surdutovich, and V. P. Yakovlev, *Mechanical Action of Light on Atoms* (World Scientific, Singapore, 1990).
[4] H. Metcalf and P. van der Straten, Phys. Rep. **244**, 203 (1994).
[5] S. Chu, J. E. Bjorkholm, A. Ashkin, and A. Cable, Phys. Rev. Lett. **57**, 314 (1986).
[6] Y. Torii, N. Shiokawa, T. Hirano, Y. Shimizu, and H. Sasada, Eur. Phys. J. D **1**, 239 (1998).
[7] L. Allen, M. W. Beijersbergen, R. J. C. Spreeuw, and J. P. Woerdman, Phys. Rev. A **45**, 8185 (1992).
[8] M. Babiker, W. L. Power, and L. Allen, Phys. Rev. Lett. **73**, 1239 (1994).
[9] W. L. Power, L. Allen, M. Babiker, and V. E. Lembessis, Phys. Rev. A **52**, 479 (1995).
[10] N. B. Simpson, K. Dholakia, L. Allen, and M. J. Padgett, Opt. Lett. **22**, 52 (1997).
[11] A. T. O'Neil and M. J. Padgett, Opt. Commun. **193**, 45 (2001).
[12] M. Soljačić and M. Segev, Phys. Rev. Lett. **86**, 420 (2001).
[13] D. S. Bradshaw and D. L. Andrews, Phys. Rev. A **72**, 033816 (2005).
[14] D. S. Bradshaw and D. L. Andrews, Opt. Lett. **30**, 3039 (2005).
[15] L. Allen, M. Babiker, W. K. Lai, and V. E. Lembessis, Phys. Rev. A **54**, 4259 (1996).
[16] A. R. Carter, M. Babiker, M. Al-Amri, and D. L. Andrews, Phys. Rev. A **73**, 021401(R) (2006).
[17] C. J. Pethick and H. Smith, *Bose-Einstein Condensation in Dilute Gases* (Cambridge University Press, Cambridge, 2002).
[18] A. Gray, *Modern Differential Geometry of Curves and Surfaces with Mathematica*, 2nd ed. (CRC Press, Boca Raton, FL, 1997).
[19] *The Physics of Quantum Information*, edited by D. Bouwmeester, A. Ekert, and A. Zeilinger (Springer, Berlin, 2000).
[20] H. C. Nägerl *et al.*, in *The Physics of Quantum Information* (Ref. [19]), p. 163.